

Preferred citation: P.R. McKinlay. Analysis of the strain field in a twisted sandwich panel with application to determining the shear stiffness of corrugated fibreboard. In **Products of Papermaking**, *Trans. of the Xth Fund. Res. Symp. Oxford, 1993*, (C.F. Baker, ed.), pp 575–599, FRC, Manchester, 2018. DOI: 10.15376/frc.1993.1.575.

**ANALYSIS OF THE STRAIN FIELD IN A TWISTED SANDWICH PANEL
WITH APPLICATION TO DETERMINING THE SHEAR STIFFNESS OF
CORRUGATED FIBREBOARD**

P R McKinlay.,
Amcor Research and Technology Centre.
P.O.Box 1
Fairfield 3078
AUSTRALIA

Abstract

Accurate measurement of the shear stiffness of corrugated fibreboard and other high performance sandwich panels is difficult because most loading strategies required to introduce shear stresses also introduce secondary effects, which complicate the measurement.

This paper analysis the strain field introduced by twisting a strip of material and demonstrates a simple relationship for accurately determining the shear stiffness of corrugated fibreboard and other high performance sandwich panels.

INTRODUCTION

The simplest type of sandwich panel consists of two stiff, high strength sheets (or facings) separated by a low density core.

This construction has been used in many engineering applications to create high performance, cost effective structures found in building construction, aircraft and more commonly in packaging.

The purpose of the facings is to provide high bending stiffness to the panel and protection to the easily damaged core. The purpose of the core is to provide facing separation without undue weight penalty, to provide sufficient shear stiffness compatible with the overall bending stiffness of the panel, and provide lateral support to the facings to inhibit local buckling instability.

Any damage to the core material by excessive lateral pressure can severely weaken the core structure. This is particularly true of a corrugated core (Fig 1) used extensively in packaging applications.

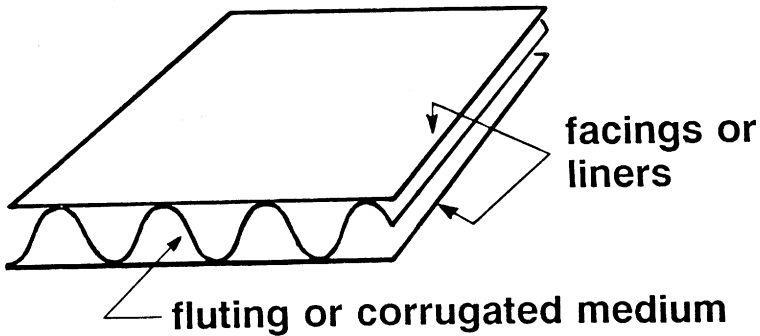


Figure 1. Panel with a corrugated core.

Lateral pressure, especially if localised, causes crushing and permanent deformation to the fluted corrugations with consequent drastic loss in machine direction (MD) shear stiffness of the core. In the packaging field in particular, low cost methods of measuring and controlling shear damage to corrugated panels is of particular importance.

This paper examines the fundamental relationship between the MD shear stiffness of sandwich panels by measurement of the twisting stiffness of long strip samples.

In particular this analysis examines corrugated core structures, representing the more complicated case. However, the techniques explained here are also applicable to sandwich panels of solid core construction.

Definition of MD Shear Stiffness

Shear stiffness is a fundamental structural property of a sandwich panel and is defined by

$$D_o = \frac{Q}{\gamma} \quad (1)$$

where Q is the MD shear force on the panel per unit width (kN/m), γ is the shear strain and D_o is the MD shear stiffness (kN/m). Details of geometry are shown in Fig 2, where h is the distance between the mid plane of the facings. For a corrugated core, p is the pitch of the corrugations.

Relationship between MD Shear Stiffness and Twisting Stiffness

Pure shear deformation, described in the previous section is difficult to achieve in practice without introducing spurious boundary conditions, which complicate attempts to accurately measure the true shear stiffness (1-2). If bending techniques are used to measure shear, the bending deflections dominate and it is difficult to accurately isolate the

shear component from the total deflection.

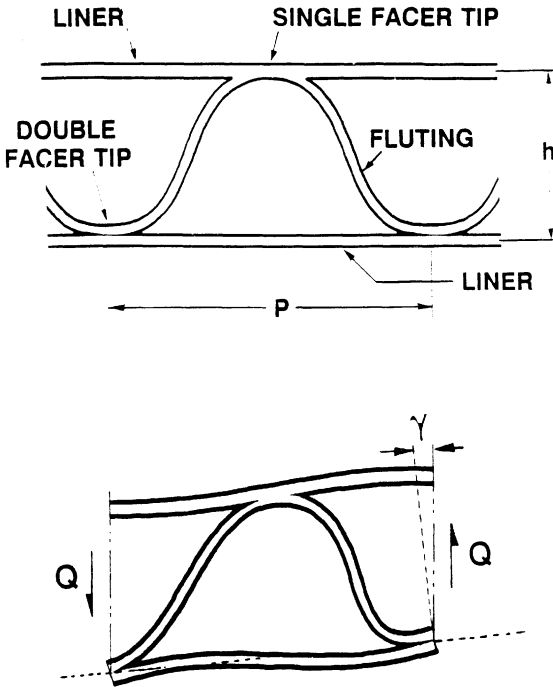


Figure 2. Geometry of the fluting cross section, in the undeformed state, and under machine direction (MD) shear.

However, by twisting a long strip sample of the panel material, it is possible to introduce large shear deflections in the core of the panel, but without large shear strains occurring in the facings, because these are always relatively stiff (Fig 3). Obviously the total twisting stiffness is a parallel combination of twisting stiffness from the liners and the core. If the angle of twist is kept sufficiently small, non linear twisting moments that develop in the liners under large deflections can be neglected. Also for simplicity of analysis the twisting moments of the liners themselves

have been assumed negligible. This will be a good approximation if the liners are thin relative to the panel thickness h , and the amount of twist is kept small. In any case these twisting moments can be easily calculated from first principles and added to the analysis.

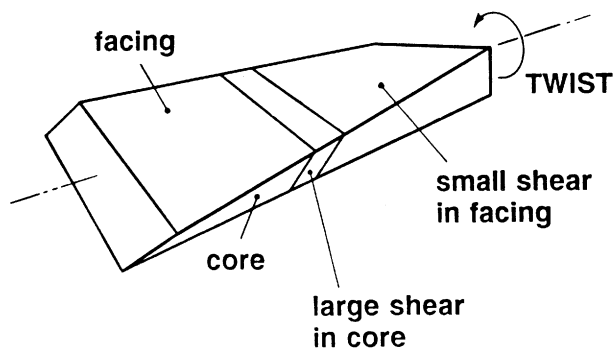


Figure 3. A twisted strip, which introduces shear strains into the core.

The main issue to be resolved is how to handle the complicated geometry introduced by twisting and relate this back to a force balance in the structure, in terms of the shear stiffness of the core and liner materials. This will be done in the following sections.

METHOD

In the development of this work, the basic approach has been to combine the capability of differential geometry (3-5) and its powerful techniques for describing twisted and curved surfaces, with the perhaps more familiar discipline of continuum mechanics (6). The notation used here is chosen to be consistent with the above references.

Adopting a differential geometry approach allows an intuitive (and satisfying) visualisation of the displacement field, such that an orthogonal grid aligned with the undeformed sample is transformed (or mapped) into a distorted grid.

For example, it is easy to visualise the liner as being under shear between the flute tips, with a resisting moment required at the flute tip to maintain equilibrium under this shear loading. The boundary conditions are that of a cantilever beam as shown in Figure 4. In this picture the undeformed liner is shown dotted and the deformed grid is shown in heavy lines.

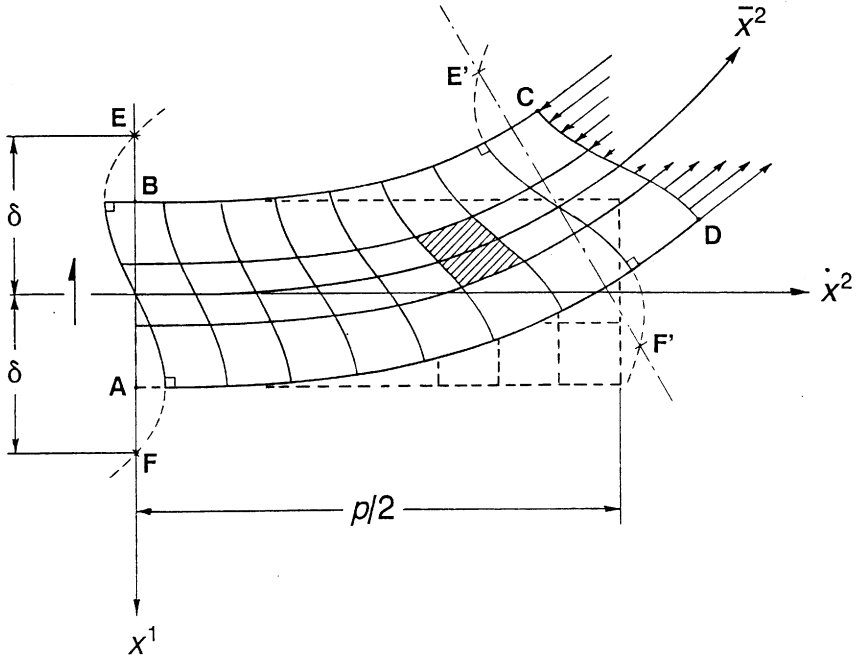


Figure 4. The liner displacement field, under a shearing action between the flute tips at $x^2 = \pm p/2$.

Under shearing stresses, a vertical line of the undeformed grid becomes curved. Consider for example the line AB, corresponding to the undeformed points at $x^2 = 0$. Also observe that shear stresses will distort rectangles into parallelograms, (shown shaded), as in evidence along the \bar{x}^2 centre line. Thus \bar{x}^2 , the displaced location corresponding to x^2 , must

be an odd function in x^1 , and meet the edge of the liner at right angles, as no shear is possible at an edge. The simplest function that meets this criteria is a cubic expression, which is anti symmetric about $x^1 = 0$, (that is, becomes zero at x^1 equal to $\pm\delta$ at points E and F, where δ can be chosen to ensure zero shear at the liner edge). The amount of shear introduced by this expression can be adjusted by a suitable scaling factor γ , to be determined.

Notice that in moving toward the flute tip (line CD), the cubic curve introduced above must rotate, so that line E'F' remains orthogonal to the facing centre line (\bar{x}^2 axis). This can be allowed by introducing an α term, such that the rotation increases in proportion to $(x^2)^2$, this being the gradient of the \bar{x}^2 axis.

The distorted field of Figure 4 must be mapped onto a twisted surface, as the liner itself is twisted. Continuity of cross sections in the vertical x^1, x^3 plane may require that this whole field be rotated in the x^1, x^2 plane. Such rotation can be allowed, by introducing a suitable rotation factor, ψ .

When shear is allowed in the core, it is found that the points F,A,B and E do not necessarily lie on the x^1 axis, but must be displaced from it by a βx^1 term, so that vertical sections through the x^1, x^2 origin are now twisted by a factor β .

By the means illustrated above, all the necessary displacement and continuity requirements can be visualised independently, and combined together as required to specify the complete displacement field, in terms of unknown constants. This will be done in a more formal way in the following sections.

Finally, these constants are determined, such that the overall boundary and force equilibrium conditions within the twisted sample are satisfied, at least globally.

SHEAR TWIST ANALYSIS

Consider in Figure 5 a coordinate system x^i aligned with the axis of symmetry of an untwisted shear twist sample of width w and thickness h .

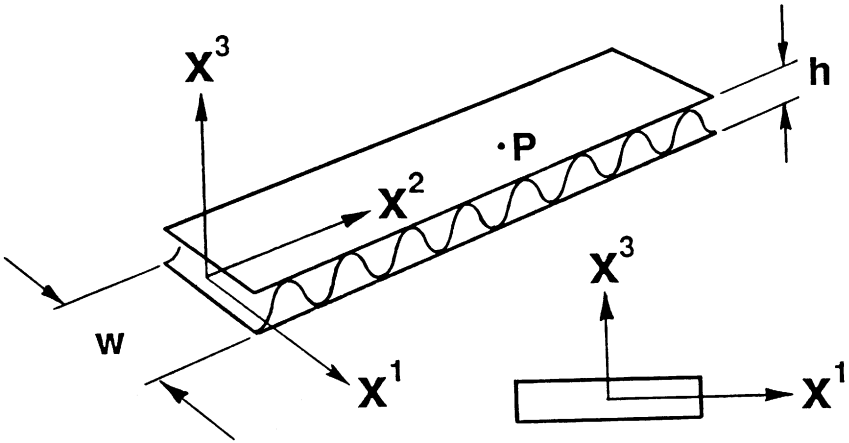


Figure 5. Geometry of the undeformed sample.

The sample is twisted by rotation about the x^2 axis, (Fig 6). Point P in the untwisted sample, located by the vector (x^1, x^2, x^3) , moves with the twisted material to a new location \bar{P} defined by the vector $\mathbf{r} = (\bar{x}^1, \bar{x}^2, \bar{x}^3)$. Point P is mapped to point \bar{P} by the equations (1) - (3) as follows.

$$\bar{x}^1 = x^1 \cos(kx^2) - x^3 \sin(kx^2) + \phi x^3 (x^2)^3 + \psi x^2 x^3 + \zeta (x^1)^2 x^2 x^3$$

$$\bar{x}^2 = x^2 + [\beta x^1 - \alpha x^1 (x^2)^2 - \gamma x^1 (\delta - x^1) (\delta + x^1)] x^3 - \psi x^1 x^3 \quad (1) - (3)$$

$$\bar{x}^3 = x^1 \sin(kx^2) + x^3 \cos(kx^2)$$

The above mapping is chosen to satisfy the required equilibrium and boundary conditions of the liners under the twisting action, as discussed in the previous section, over the range $x^1 = \pm w/2$, $x^2 = \pm p/2$, $x^3 = \pm h/2$. Here k is the rotation per unit length in the x^2 direction and ϕ ψ α β δ γ and ζ are constants to be determined by equilibrium of forces within the structure.

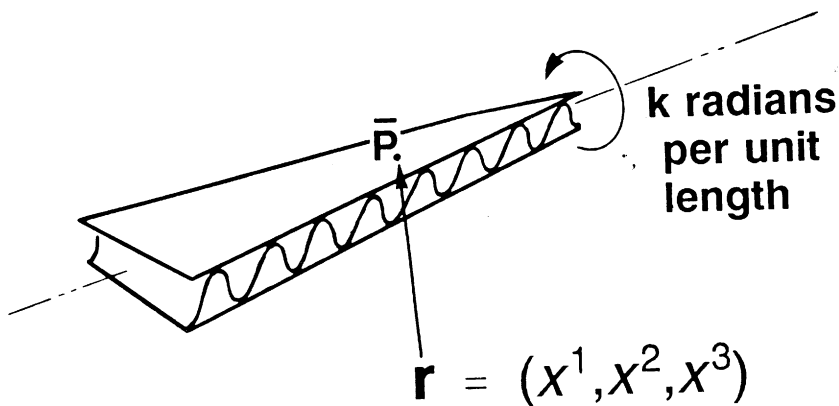


Figure 6. Location of material in the twisted sample.

Note that flute tips (glue lines) are assumed to be located at $x^2 = \pm p/2$ on both facings, which is not strictly true for corrugated board. There is no loss of generality in this assumption however, as symmetry allows the deflected shapes above and below the $x^3 = 0$ plane to be shifted by half a flute pitch, to satisfy the requirements for the corrugated board case.

The liners of the sample are distorted under the twisting action with local changes in geometry defined by the metric g_{ij} as follows:

$$\mathbf{r}_i = \frac{\partial \mathbf{r}}{\partial x^i} \quad (4)$$

$$g_{ij} = \mathbf{r}_i \cdot \mathbf{r}_j \quad (5)$$

Deformation of the twisted sample is specified by the strain tensor ε_{ij} defined as

$$\varepsilon_{ij} = \frac{1}{2}(g_{ij} - \delta_{ij}) \quad (6)$$

To a first order approximation it can be shown, by applying equations (4) and (5) that

$$g_{11} = 1 + 4\zeta x^1 x^2 x^3 \quad (7)$$

$$g_{12} = \{ (3\phi - a)(x^2)^2 - \nu[\delta^2 - 3(x^1)^2] + \zeta(x^1)^2 + \beta - k \} x^3 \quad (8)$$

$$g_{13} = \{ \psi + \phi(x^2)^2 + \zeta(x^1)^2 \} x^2 \quad (9)$$

$$g_{22} = 1 - 4ax^1 x^2 x^3 \quad (10)$$

$$g_{23} = \{ \beta - \psi - a(x^2)^2 - \nu[\delta^2 - (x^1)^2] + k \} x^1 \quad (11)$$

$$g_{33} = 1 \quad (12)$$

Liner Boundary Conditions

In analysing the stress/strain field in the liner ($x^3 = \pm h/2$), the simplifying assumptions are made of :-

1. Small strains.
2. Plane stress.
3. Orthotropic material properties.

Under these assumptions, the compatibility equations (6), which ensure a continuous and single valued displacement field, have already been satisfied by a sensible choice of functions, equations (1) to (3).

For equilibrium of forces in the plane of the liner, the equation to be satisfied is

$$\sigma_{ij,j} = 0 \quad (13)$$

Solution of the compatibility and equilibrium equations are often obtained through use of the Airy stress function (6). It is evident that at the edge of the facings ($x^1 = \pm w/2$), both the tensile stress σ_{11} and the shear stress σ_{12} are zero. Examination of suitable Airy stress functions shows that these boundary conditions are satisfied with $\sigma_{11} = 0$ everywhere, and a shear stress distribution which is parabolic in x^1 and invariant with respect to x^2 .

In a plane stress situation it is convenient to use a contracted, but obvious notation for the elastic modulus. ($E_{1111} = E_{11}$, $E_{1122} = G_{12}$ etc.) Thus under conditions of plane stress

$$\sigma_{11} = \frac{E_{11}}{g} (\epsilon_{11} + \nu_{2211} \epsilon_{22}) \quad (14)$$

where E_{11} is the elastic modulus of the liner in the CD (cross machine direction), and $g = 1 - \nu_{1122}\nu_{2211}$.

The strains ε_{11} and ε_{22} can be found by applying equation (6) to equations (7) and (10), giving

$$\varepsilon_{11} = 2 \zeta x^1 x^2 x^3 \quad (15)$$

$$\varepsilon_{22} = -2 \alpha x^1 x^2 x^3 \quad (16)$$

therefore

$$\sigma_{11} = \frac{2E_{11}}{g} (\zeta - \nu_{2211}\alpha) x^1 x^2 x^3 \quad (17)$$

Now as already indicated, the boundary conditions within the liners ($x^3 = \pm h/2$) can only be satisfied with $\sigma_{11} = 0$ everywhere. This gives, by equation (17)

$$\zeta = \nu_{2211}\alpha \quad (18)$$

Applying equation (13) in the x^1 direction ($i=1$) gives

$$\sigma_{11,1} + \sigma_{12,2} = 0 \quad (19)$$

Now as $\sigma_{11} = 0$ everywhere, $\sigma_{11,1} = 0$ which implies that $\sigma_{12,2} = 0$.

This means σ_{12} and therefore g_{12} can not be a function of x^2 . Thus from equation (8)

$$\alpha = 3\phi \quad (20)$$

Also at the edge of the liner ($x^1 = \pm w/2$, $x^3 = \pm h/2$) shear stresses are zero, that is

$$\sigma_{12} = g_{12} = 0$$

Therefore from equation (8)

$$\beta - k - \gamma\delta^2 = -(3\gamma + \zeta) \left(\frac{w}{2} \right)^2 \quad (21)$$

This gives, in the general case, after substituting equations (20) and (21) into (8),

$$g_{12} = -(3\gamma + \zeta) \left\langle \left(\frac{w}{2} \right)^2 - (x^1)^2 \right\rangle x^3 \quad (22)$$

Liner equilibrium in the x^2 direction, ($i=2$ in equation (13)) gives

$$\sigma_{21,1} + \sigma_{22,2} = 0 \quad (23)$$

Now

$$\begin{aligned} \sigma_{12} &= \sigma_{21} = G_{12}\gamma_{12} \\ &= G_{12}g_{12} \end{aligned}$$

where $\gamma_{ij} = 2\varepsilon_{ij} = g_{ij}$

and G_{12} is the in-plane shear modulus of the liners. Therefore

$$\sigma_{12} = -(3\gamma + \zeta)G_{12} \left\langle \left(\frac{w}{2} \right)^2 - (x^1)^2 \right\rangle x^3 \quad (24)$$

and

$$\sigma_{21,1} = 2(3\gamma + \zeta)G_{12}x^1x^3 \quad (25)$$

Also

$$\sigma_{22} = \frac{E_{22}}{g}(\epsilon_{22} + \nu_{1122}\epsilon_{11}) \quad (26)$$

where E_{22} is the elastic modulus of the liners in the x^2 direction.

Substituting equations (15) and (16) into the above equation gives,

$$\sigma_{22} = \frac{2E_{22}}{g}(\nu_{1122}\zeta - \alpha)x^1x^2x^3 \quad (27)$$

but substituting for ζ from equation (18) finally gives

$$\sigma_{22} = -2\alpha E_{22}x^1x^2x^3 \quad (28)$$

Differentiating σ_{22} gives

$$\sigma_{22,2} = -2\alpha E_{22}x^1x^3 \quad (29)$$

Substituting equations (18), (25) and (29) into (23) gives

$$\frac{\alpha E_{22}}{3\gamma G_{12}} = \frac{E_{22}}{E_{22} - \nu_{2211}G_{12}} = \rho \quad (30)$$

As the sample twists, symmetry requires that cross sections defined by the x^1x^3 plane and passing through a flute tip can not

undergo shear along the cross section centre lines. This requires that $g_{13} = 0$ at $x^1 = 0, x^2 = p/2$ where p is the pitch of the flutes.

Applying this condition to equation (9) and using equation (20) gives

$$\psi = -\frac{\alpha}{3} \left(\frac{p}{2} \right)^2 \quad (31)$$

Equilibrium of the Glue Line

The glue line is in equilibrium under the action of forces from the liner and medium.

Consider moments on the glue line (at $x^2 = p/2$) arising from forces on the liner segment ABCD, (Fig 7).

Along lines AB and CD (at $x^2 = 0, p$), σ_{11} and σ_{22} make no nett contribution to moments about E because of symmetry. Thus the total moment on the glue line from the liner at $x^3 = +h/2$ (defining anti clockwise rotation positive), is

$$M_L = -t \int_{-\frac{w}{2}}^{\frac{w}{2}} \sigma_{12} p dx^1 = -2t \int_0^{\frac{w}{2}} \sigma_{12} p dx^1 \quad (32)$$

where t is the thickness of the liner. Substituting equation (24) into the above and integrating gives

$$M_L = \frac{\gamma w^3}{4} t G_{12} p h e \quad (33)$$

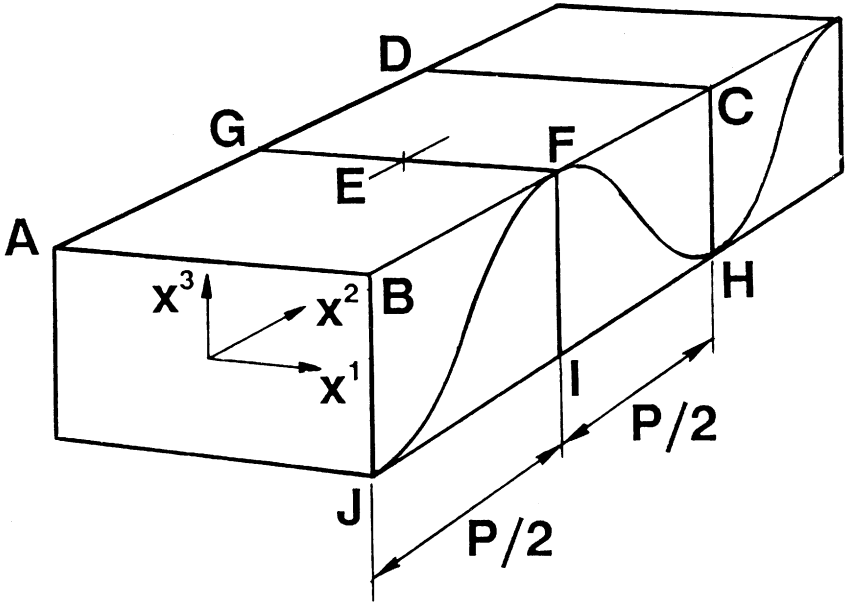


Figure 7. Location of the glue line connecting fluting and liner.

Consider now forces on the glue line from the medium, (Fig 7). We can examine a section BCHJ at the edge ($x^1 = w/2$) or at any other x^1 value. The rectangle BCHJ will be distorted to a parallelogram B'C'H'J' as shown in Figure 8. A section of width dx^1 under shear forces dQ will develop a shear strain, designated γ_{23} .

Under these pure shear conditions (the two dimensional case) the shear stiffness is defined as

$$D_Q = \frac{Q}{\gamma_{23}} = \frac{Q}{g_{23}} \quad (34)$$

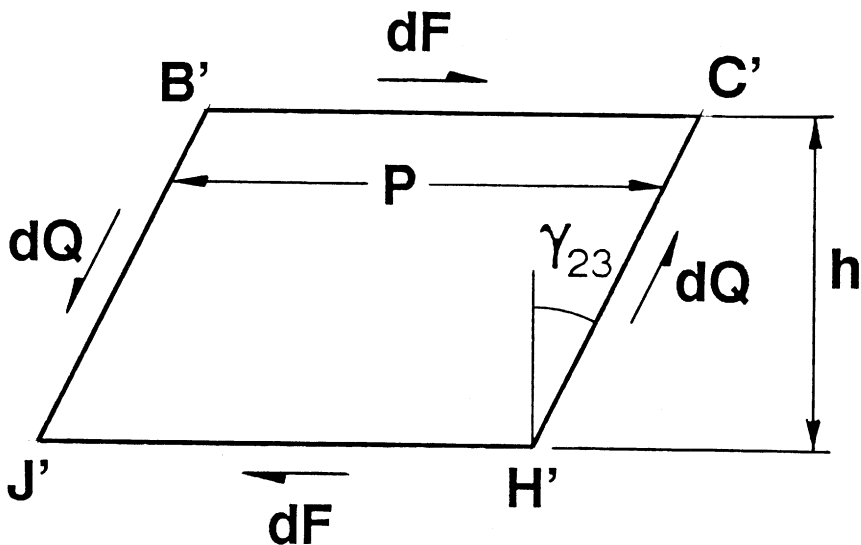


Figure 8. Shear in the fluting (corrugating medium).

Also for equilibrium of the section $h dF = p dQ$ where, $dQ = Q dx^1$

Thus

$$dF = \frac{p}{h} g_{23} D_a dx^1 \quad (35)$$

In the three dimensional case the forces dF must be transferred to the glue line. There may be other forces acting which contribute to dF but these are small if rotation k is kept sufficiently small. Thus the moment on the glue line, defined by the vector $(x^1, p/2, h/2)$, is

$$\begin{aligned}
 M_M &= \int_{-\frac{w}{2}}^{\frac{w}{2}} x^1 dF \\
 &= 2 \frac{\rho}{h} D_o \int_0^{\frac{w}{2}} (g_{23})_{x^2 = \frac{\rho}{2}} x^1 dx^1
 \end{aligned} \tag{36}$$

From equation (11) and applying the appropriate boundary conditions using equations (21) and (30), g_{23} can be expressed in terms of γ and k only.

Substituting into (36) and integrating gives

$$M_M = \frac{w^2 \rho D_o (\gamma w^3)}{4h} \left[\frac{A}{3 \gamma w^2} + \frac{1}{20} \right] \tag{37}$$

where

$$A = 2k - \gamma C \tag{38}$$

and

$$C = 3 \left[\frac{w}{2} \right]^2 + \rho \frac{G_{12}}{E_{22}} \left\langle 2 \left[\frac{\rho}{2} \right]^2 + 3 \nu_{2211} \left[\frac{w}{2} \right]^2 \right\rangle \tag{39}$$

For glue line equilibrium, taking moments about the x^3 axis, requires $M_L = M_M$. This requires, after simple manipulation that

$$\gamma w^3 = \frac{2Aw}{3 \left\langle \frac{2\rho t G_{12}}{D_o} \left[\frac{h}{w} \right]^2 - \frac{1}{10} \right\rangle} \tag{40}$$

Moment of Twist

To twist the sample requires a moment M . Consider the forces

on the liners as shown in Figure 9.

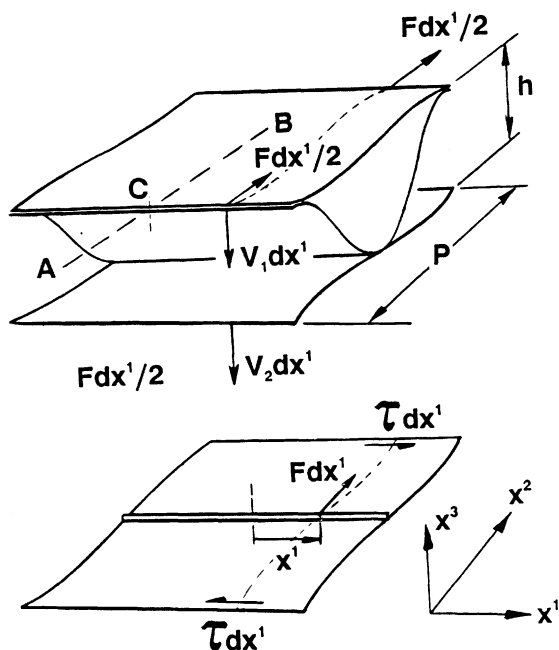


Figure 9. Moment equilibrium about the x^2 axis.

Assuming elemental widths behave as if in pure shear, we conclude that

$$Fh = (V_1 + V_2)\rho \quad (41)$$

Also for equilibrium of the liner

$$\int_{-\frac{w}{2}}^{\frac{w}{2}} F x^1 dx^1 = t \int_{-\frac{w}{2}}^{\frac{w}{2}} \tau \rho dx^1 \quad (42)$$

where τ is the shear field in the liner, which varies in the x^1 direction but not in the x^2 direction. Moments about AB in a vertical plane through C requires

$$M = \int_{-\frac{w}{2}}^{\frac{w}{2}} (V_1 + V_2) x^1 dx^1 + ht \int_{-\frac{w}{2}}^{\frac{w}{2}} \tau dx^1 \quad (43)$$

The first integral in (43) above can be simplified, by substituting (41) and then (42) to give

$$M = 2ht \int_{-\frac{w}{2}}^{\frac{w}{2}} \tau dx^1 \quad (44)$$

Now $\tau = -\sigma_{12}$ and is symmetrical in x^1 , therefore

$$M = -4ht \int_0^{\frac{w}{2}} \sigma_{12} dx^1 \quad (45)$$

Substituting equation (24) into the above and integrating gives

$$M = \frac{\gamma w^3}{2} t G_{12} h^2 \varrho \quad (46)$$

Substituting for γw^3 from equation (40) gives

$$M = \frac{\varrho t G_{12} h^2 A w}{3 \left\langle \frac{2\varrho t G_{12}}{D_a} \left[\frac{h}{w} \right]^2 - \frac{1}{10} \right\rangle} \quad (47)$$

Expressing the moment M per unit twist k , in terms of shear units,

by the equation

$$D_{aM} = \frac{M}{kW^3} \quad (48)$$

it can be shown, using equations (40), (47) and (48) that

$$\frac{D_a}{D_{aM}} = 3 + \{1 + a + b\} \frac{3D_a}{5tG_{12}} \left[\frac{w}{h} \right]^2 \quad (49)$$

where

$$a = \frac{G_{12}}{E_{22}} \frac{v_{2211}}{4}, \quad b = \frac{5}{6} \frac{G_{12}}{E_{22}} \left[\frac{p}{w} \right]^2 \quad (50)$$

For corrugated board, the term a is a ratio of paper properties and is a small constant, typically 0.028.

The term b is generally small (around 0.018 for C flute) and can be disregarded for sample dimensions such that $w > 3p$ typical of commercial corrugated boards used in packaging, and where the sample width has been chosen to be 25 mm.

Equation (49) establishes a fundamental but simple relationship between the shear twist test and the MD shear stiffness of corrugated board. It allows measurements from a shear twist instrument to determine pure MD shear stiffness accurately, irrespective of the choice of liner weight.

CONFIRMATION OF ANALYSIS USING FINITE ELEMENT METHODS

The Finite Element Method has been used to confirm in detail the validity of the mathematical analysis.

Four node shell elements (ABAQUS S4R5) were used, comparing

coarse and fine meshes to check convergence.

Two sets of boundary conditions were applied to the models. One set applied a pure MD shear displacement, thereby determining D_Q ; the other a rotation about the MD (x^2) axis to determine D_{QM} . Results were compared using equation (49).

Two types of glue modelling were also used to connect the liners to the medium. In one case multi point constraints (MPC's) were used. In the other, the tips of the medium were joined to the liners using short shell elements. As expected, a more rigid glue connection gives a higher shear stiffness.

In order to increase the accuracy of the finite element model, only one flute cell was modelled. Boundary conditions were chosen to simulate a series of connected and continuously twisting cells, compatible with an infinitely long sample.

Finite element results are summarised in figure 10, compared to the analytical work, equation (49). A detailed examination of the strain field predicted by the finite element method confirms that the first order approximations assumed in the analytical work are adequate, provided rotation of the twisted sample is kept in the linear range.

The results show a simple linear relationship, covering a wide commercial range of liners (115-300 g/m².) and C flute mediums (115-230 g/m².), demonstrating the linear form of equation (49), and confirming the fundamental relationship that exists between MD Shear Stiffness and the twisting stiffness of a strip of corrugated board. For liner and fluting combinations in reasonable balance, suitable in commercial applications, the difference between the analytical and finite element results is under ten percent. In situations where shear stiffness is low, such that overall performance of the corrugated structure might be compromised, the results fall towards the left of the graph. In this case the difference between the results is around six percent.

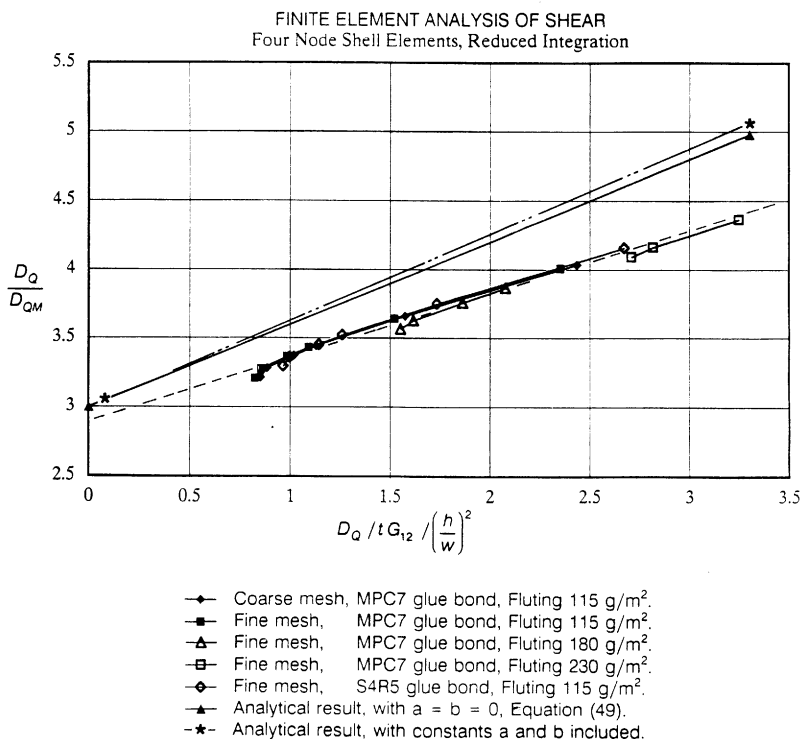


Figure 10. Comparison of analytical and finite element results.

CONCLUSION

A simple analytical relationship has been shown between the MD shear stiffness of a sandwich panel and the twisting stiffness of a long strip sample. This relationship is of a form which allows correction for the effect of the liners on the twisting stiffness, to arrive at a true measure of the MD shear stiffness of corrugated panels. The same method is

applicable to sandwich panels with a solid core construction.

Finite element analysis confirms the analytical results for the corrugated board case.

The twist method therefore provides a reliable and accurate way to test the quality of sandwich panel construction. This is particularly relevant to the manufacture and quality control of corrugated fibreboard structures used extensively in the packaging industry.

ACKNOWLEDGMENT

The author would like to thank AMCOR LTD and AMCOR Fibre Packaging for their support over many years in funding research and development work on corrugated fibreboard structures.

REFERENCES

1. Allen, H.G., "Measurement of Shear Stiffness of Sandwich Beams," *Trans. J. Plastics Inst*, 35, (Feb 1967) pp. 359-363.
2. Adams, R.D. and Weinstein, A.S., "Flexural Stiffness of Sandwich Beams," *Journal of Engineering Materials and Technology*, *Trans of the ASME*, (July 1975) pp. 264-270.
3. B. F. Schutz., "Geometrical Methods of Mathematical Physics," Cambridge University Press, (1980).
4. M. Nakahara., "Geometry, Topology and Physics," Adam Hilger, Bristol, (1990).
5. C. T. J. Dodson, and T. Poston., "Tensor Geometry: The Geometric Viewpoint and its Uses," 2nd ed., Springer-Verlag, (1990).
6. W. Flügge., "Tensor Analysis and Continuum Mechanics," Springer-Verlag, (1972)

Transcription of Discussion

ANALYSIS OF THE STRAIN FIELD IN A TWISTED SANDWICH PANEL WITH APPLICATIONS TO DETERMINING THE SHEAR STIFFNESS OF CORRUGATED FIBREBOARD

P R McKinlay

Dr C Fellers, STFI, Sweden

When you derive the equations for the box performance I notice that you are using time independent elastic properties. When you model a box can you include also a time dependence somewhere in the equations. Could you extend the model using the isochronous stress-strain curves?

P McKinlay

Yes. You have the facility to twist the sample and hold and get a relaxation. You can put a constant moment and get a creep. Translating it into information including time is very easily done.

D Gunderson, US Dept of Agriculture, USA

Does the mathematical analysis explain the dimpled appearance? In the beginning you showed us dimples - the microbuckling that goes between the flute lines. Does the mathematical analysis explain the presence of those?

P McKinlay

No. The only point I was making there was as these micropanels develop, they are tied to the fluting underneath so the stiffness of the fluting is helping maintain that lateral stability. So when we get a

micropanel field develop an important part of the development of that field is how well we can stabilise the facing against lateral buckling. So it is an important part of box compression behaviour which up till now has not been correctly taken into account.

Dr S Loewen, Abitibi-Price Inc, Canada

Your finite element model looks as if it could be quite powerful for optimising the different component properties such as the liner or the board in terms of stiffness or strength properties. Have you used it for that?

P McKinlay

We will be pursuing that route. Until now I have built a model of box compression behaviour based on orthogonal polynomial displacement field and we have been using that model as a basis for prediction which has worked out very well. We have been able to satisfy our needs up to now with that model, but there are a lot of things that are happening which we cannot predict and that is where the finite element model comes into its own. It will be very important in the description of material behaviour. I make the point that what we have shown here in terms of differential geometry, it has taken 150 years for physicists to catch up. We have a very powerful tool and this is one simple example of how it could be used but we are dealing with geometry and we can make great progress if we start to use the tools that we have.